Inorg. Chem. **2002**, *41*, 6322–6331

4-Hydroxypyridine-2,6-dicarboxylatodioxovanadate(V) Complexes: Solid State and Aqueous Chemistry

Luqin Yang,† Agnete la Cour, Oren P. Anderson, and Debbie C. Crans*

Department of Chemistry, College of Natural Sciences, Colorado State University, Fort Collins, Colorado 80523

Received February 27, 2002

The aqueous solution and solid state properties of (4-hydroxypyridine-2,6-dicarboxylato)dioxovanadate(V) (also referred to as (4-hydroxydipicolinato)dioxovanadate(V) or (chelidamato)dioxovanadate(V) and abbreviated $[VO_2(dipic\text{-}OH)]^-$) were investigated. By using ^1H, ^{13}C, ^{17}O, and ^{51}V NMR 1D and 2D spectroscopy, the species present in solution, together with pK_a values, equilibrium constants, and labilities, were characterized. The complex is most stable at acidic pH down to pH 1 where it is protonated. The stability of this complex is higher than that of the parent dipicolinatodioxovanadate(V) complex. The dipic-OH ligand is coordinated in a tridentate manner throughout the pH range studied, and the vanadium(V) atom is five-coordinate. Solid state structures of $(NMe_4)[VO_2(dipic\text{-}OH)]\cdot H_2O$ (monoclinic, $P2_1/n$) and $Na[VO_2(dipic\text{-}OH)]\cdot 2H_2O$ (triclinic, $P\bar{1}$) were determined. The discrete complex anions in $(NMe_4)[VO_2(dipic\text{-}OH)]\cdot H_2O$ are connected by hydrogen bonding between the hydroxyl group, a water molecule, and a carboxylate oxygen atom. Changing the counterion from NMe_4^+ to sodium ion in $Na[VO_2(dipic\text{-}OH)]\cdot 2H_2O$ leads to the formation of a polymeric structure. Dynamic processes in solution were explored by using ^1H and ^{13}C EXSY NMR spectroscopy; exchange between complex and free ligand below pH 4 was observed. The differences between the dipicolinatodioxovanadate(V) parent complex and the $[VO_2(dipic\text{-}OH)]^-$ complex in the solid state and in solution demonstrate the subtle consequences of the one substitutional difference between the two ligands. The insulin-mimetic properties of this compound are likely to be of mechanistic interest in developing an understanding of the mode of action of the few known insulin-mimetic vanadium(V) complexes.

Introduction

There has been increasing interest in the fundamental coordination chemistry of vanadium compounds, due to the fact that a vanadium(IV) compound, KP-102,[1,2] is in clinical trials as a potential treatment for non-insulin-dependent diabetes mellitus (NIDDM). A vanadium(V) complex, dipicolinatodioxovanadium(V) (dipicolinate = pyridine-2,6-dicarboxylate), was recently shown to have insulin-mimetic properties.[3–6] This compound is the first well-characterized vanadium(V) complex that has proven active in vivo, although a less well characterized vanadium(V) complex involving a modified dipeptide hydroxamate has also shown promise.[7] We are interested in the characterization of new related vanadium compounds, in part because such compounds may provide mechanistic information with regard to how such complexes act in biological systems. Although many metal complexes of dipicolinic acid have been described, the transition metal complexes of modified dipicolinates have been less well studied. In this work we describe a new vanadium(V) complex that contains 4-hydroxypyridine-2,6-dicarboxylic acid (chelidamic acid, H_2-dipic-OH).

The acid−base differences between the ligands H_2dipic and H_2dipic-OH are well-established. H_2dipic contains two

* Author to whom correspondence should be addressed. E-mail: crans@lamar.colostate.edu. Phone: (970) 491-7635. Fax: (970) 491-1801.

† Permanent address: Department of Chemistry, Peking University, Beijing, China.

(1) McNeill, J. H.; Yuen, V. G.; Hoveyda, H. R.; Orvig C. *J. Med. Chem.* **1992**, *35*, 1489−1491.
(2) Thompson, K. H.; McNeill, J. H.; Orvig, C. *Chem. Rev.* **1999**, *99*, 2561−2571.
(3) Fondacaro, J. V.; Greco, D. S.; Crans, D. C. *Annu. Vet. Med. Forum* **1999**.
(4) Crans, D. C.; Yang, L.; Alfano, J. A.; Chi, L.-H.; Jin, W.; Mahroof-Tahir, M.; Robbins, K.; Toloue, M. M.; Chang, L.; Plante, A. J.; Grayson, R.; Willsky, G. R. *Coord. Chem. Rev.*, in press.
(5) Plottnick, A. N.; Greco, D. S.; Crans, D. C.; Elfrey, S. *Proc. Annu. Vet. Med. Forum* **1995**, *5*.
(6) (a) Greco, D. S.; Crans, D. C. *J. Inorg. Biochem.*, submitted. (b) Crans, D. C. *J. Inorg. Biochem.* **2000**, *80*, 123−131.
(7) Goldwasser, I.; Li, J.; Gershonov, E.; Armoni, M.; Karnieli, E.; Fridkin, M.; Shechter, Y. *J. Biol. Chem.* **1999**, *274*, 26617−26624.

10.1021/ic0201598 CCC: $22.00
Published on Web 11/01/2002

acidic protons, with pK_a values of 2.16 and 4.76.[8] H_2dipic-OH contains three acidic protons, with pK_a values of <2, 3.47, and 11.4.[9] The lower pK_a values for the two most acidic protons in H_2dipic-OH reflect the stabilizing effect of the hydroxyl substituent. The anticipated differences between the title complex relative to the (dipic)dioxovanadate(V) parent complex include increased potential for hydrogen bonding, increased solubility and stability in aqueous solution, a greater variety of protonation states, and possible changes in lability.

Other substituted picolinate ligands have been used previously in synthesizing vanadium complexes. For example, modifications have included methyl, ethyl, or iodo derivatives of bis(picolinato)oxovanadium(IV).[10,11] Vanadium(IV) complexes of the maltol ligand (3-hydroxy-2-methyl-4-pyrone)[12] have also been investigated, together with 2-ethyl, 2-isopropyl, and 2-*sec*-butyl derivatives.[13] Other transition metal complexes involving the chelidamic acid ligand have been reported, such as $[Cr^{III}(dipic\text{-}OH)(H_2O)(OH)]_2$[14] and $[Fe^{III}(dipic\text{-}OH)(H_2O)(OH)]_2$.[15] An important difference between those dipic-OH complexes and the $[VO_2(dipic)]^-$ and $[VO_2(dipic\text{-}OH)]^-$ complexes is the coordination number about the metal ion.

A number of vanadium(V) complexes[16,17] have recently been shown to be labile.[18−22] The complexes studied included vanadium(V) species with both monodentate[23] and polydentate O,N-donor-containing functionalities.[18,20−22,24] Some of these complexes were very stable species, and thus lability is a property associated not only with less stable vanadium complexes such as vanadium(V) alkoxides (referred to as "esters" in aqueous solution).[23] Since complex lability has been suggested to be an important property with respect to the biotransformations that occur under physiological conditions, information on the lability of other vanadium complexes with potential insulin-like activity is desirable.[6] Variable-temperature NMR studies and EXSY spectroscopic studies were employed to show that the $[VO_2(dipic)]^-$ complex was labile.[6] We have previously found that simple substitutional perturbations in organic ligands did not result in significant changes in the lability of vanadium(V) complexes,[24] and thus we expected that $[VO_2(dipic\text{-}OH)]^-$ would also be labile.[25] Surprisingly, the lability/pH profile for $[VO_2(dipic\text{-}OH)]^-$ was significantly different from that previously observed for the $[VO_2(dipic)]^-$ complex.[25] In this work, the properties of the vanadium(V) complex of H_2dipic-OH will be compared in detail to those of the complex formed with H_2dipic, both in the solid state and in solution.

Experimental Section

Materials. All reagents used were reagent grade. Water was distilled and passed over an ion-exchange column before use.

Synthesis of Na[VO_2(dipic-OH)]·2H_2O. $NaVO_3$ (1.35 g, 10.0 mmol) and H_2dipic-OH·H_2O (2.01 g, 10.0 mmol) were dissolved in hot water (30 mL). The pH of the solution was adjusted to 1.1 with 2 M HCl. After heating for 1 h, the solution was cooled and the crystalline product was isolated by filtration. The product was recrystallized from water, yielding 2.03 g (62.8%). IR (KBr, cm^{-1}): 3474 (m, br), 3209 (br, w), 3057 (m), 2750 (m), 2616 (m), 2532 (m), 1681 (vs, CO_2^-), 1611 (m), 1507 (w), 1469 (m), 1379 (vs, CO_2^-), 1295 (m), 1274 (w), 1233 (w), 1186 (w), 1130 (w), 1054 (s), 945 (vs, broad, V═O), 902 (w), 803 (s), 762 (s), 705 (w), 645 (m), 617 (w), 578 (m), 511 (w), 459 (m), 441 (w). ^{1}H NMR (D_2O, ppm, DSS): 7.565 (297 K, pH 3.05). ^{51}V NMR (D_2O, ppm, $VOCl_3$): −529.033 (297 K, pH 3.05). Calcd for $C_7H_7NO_9VNa$: C 26.01, H 2.17, N 4.33. Found: C 26.13, H 2.11, N 4.27.

Synthesis of (NMe_4)[VO_2(dipic-OH)]·H_2O. V_2O_5 (0.46 g, 2.5 mmol) and H_2dipic-OH (1.0 g, 5.0 mmol) were dissolved in water (15 mL) with heating. The pH was adjusted to 4.3 by addition of tetramethylammonium hydroxide (1.0 M, 9.0 mL, 9.0 mmol). The resulting solution was filtered while hot and then cooled to ambient temperature. A small quantity (approximately 2% yield) of colorless crystals was obtained on standing. A higher yield can be obtained by precipitation of the product with ethanol or by carrying out the reaction at a lower pH. IR (KBr, cm^{-1}): 3435 (br, s), 3053 (m), 3019 (m), 2957(w), 2922 (w), 2744 (w), 2610 (w), 2482 (w), 1681 (vs, CO_2^-), 1610 (w), 1488 (m), 1468 (w), 1380 (vs, CO_2^-), 1294 (w), 1233 (w), 1125 (w), 1055 (s), 948 (vs, broad, V═O), 803 (m), 762 (m), 578 (w), 460 (w). ^{1}H NMR (D_2O, ppm, DSS): 7.502 (py-*H*, 2H), 3.150 ($N(CH_3)_4^+$, 12H) (297 K, pH 3.27). ^{51}V NMR (D_2O, ppm, $VOCl_3$): −528.5 (297 K, pH 3.27).

Synthesis of (NMe_4)$_5${[VO_2(dipic-OH)][VO_2(dipic-O^-)]$_2$}·4H_2O. The supernatant solution remaining after the precipitation of NMe_4[VO_2(dipic-OH)]·H_2O (pH ∼ 4.3) was kept at ambient temperature for several days; during that time a pale yellow solid precipitated. This product was recrystallized from a water/ethanol mixture (about 2.5:1), yielding 56.2 mg (2.7%) of a pale yellow, hygroscopic solid. IR (KBr, cm^{-1}): 3559 (br, m), 3325 (m, sharp), 3136 (vw), 3064 (w), 1642 (vs, CO_2^-), 1612 (s), 1508 (w), 1567 (m), 1524 (s), 1512 (s), 1427 (s), 1388 (s, CO_2^-), 1320 (m), 1306

(8) Tichane, R. M.; Bennett, W. E. *J. Am. Chem. Soc.* **1957**, *79*, 1293−1296.
(9) Bag, S. P.; Fernando, Q.; Freiser, H. *Inorg. Chem.* **1962**, *1*, 887−890.
(10) Sakurai, H.; Fujii, K.; Watanabe, H.; Tamura, H. *Biochem. Biophys. Res. Commun.* **1995**, *214*, 1095−1101.
(11) Fujimoto, S.; Fujii, K.; Yasui, H.; Matsushita, R.; Takada, J.; Sakurai, H. *J. Clin. Biochem. Nutr.* **1997**, *23*, 113−129.
(12) Thompson, K. H.; Yuen, V. G.; McNeill, J. H.; Orvig, C. In *Vanadium Compounds, Chemistry, Biochemistry, and Therapeutic Applications*; Tracey, A. S., Crans, D. C., Eds.; ACS, Oxford University Press: Washington, DC, 1998; Vol. 711, pp 329−343.
(13) Thompson, K.; Orvig, C.; McNeill, J. H. Unpublished results. The data were presented at the 3rd Vanadium Chemistry and Vanadium Biochemistry Symposium in Osaka, Nov 26−29, 2001.
(14) Cline, S. J.; Kallesoe, S.; Pedersen, E.; Hodgson, D. J. *Inorg. Chem.* **1979**, *18*, 796−801.
(15) Thich, J. A.; Ou, C. C.; Powers, D.; Vasiliou, B.; Mastropaolo, D.; Potenza, J. A.; Schugar, H. J. *J. Am. Chem. Soc.* **1976**, *98*, 1425−1433.
(16) Crans, D. C.; Holst, H.; Keramidas, A. D.; Rehder, D. *Inorg. Chem.* **1995**, *34*, 2524−2534.
(17) Elvingson, K.; Keramidas, A. D.; Crans, D. C.; Pettersson, L. *Inorg. Chem.* **1998**, *37*, 6153−6160.
(18) Crans, D. C.; Ehde, P. M.; Shin, P. K.; Pettersson, L. *J. Am. Chem. Soc.* **1991**, *113*, 3728−3736.
(19) Ray, W. J., Jr.; Crans, D. C.; Zheng, J.; Burgner, J. W., II; Deng, H.; Mahroof-Tahir, M. *J. Am. Chem. Soc.* **1995**, *117*, 6015−6026.
(20) Crans, D. C.; Shin, P. K.; Armstrong, K. B. *ACS Symp. Ser.* **1995**, *246*, 303−328.
(21) Keramidas, A. D.; Miller, S. M.; Anderson, O. P.; Crans, D. C. *J. Am. Chem. Soc.* **1997**, *119*, 5447−5448.
(22) Crans, D. C.; Jiang, F.; Boukhobza, I.; Bodi, I.; Kiss, T. *Inorg. Chem.* **1999**, *38*, 3275−3282.
(23) Crans, D. C.; Schelble, S. M.; Theisen, L. A. *J. Org. Chem.* **1991**, *56*, 1266−1274.
(24) Crans, D. C.; Boukhobza, I. *J. Am. Chem. Soc.* **1998**, *120*, 8069−8078.
(25) Crans, D. C.; Yang, L.; Jakusch, T.; Kiss, T. *Inorg. Chem.* **2000**, *39*, 4409−4416.

Table 1. Crystallographic Details for $(NMe_4)[VO_2(dipic\text{-}OH)]\cdot H_2O$ and $Na[VO_2(dipic\text{-}OH)]\cdot 2H_2O$

	$(NMe_4)[VO_2(dipic\text{-}OH)]\cdot H_2O$	$Na[VO_2(dipic\text{-}OH)]\cdot 2H_2O$
empirical formula	$C_{11}H_{17}N_2O_8V$	$C_7H_7NNaO_9V$
fw	356.2	323.1
cryst syst	monoclinic	triclinic
space group	$P2_1/n$	$P\bar{1}$
lattice consts		
a, Å	11.2818(7)	5.9715(4)
b, Å	15.6422(10)	8.0069(5)
c, Å	17.3650(12)	11.7082(7)
α, deg		91.3190(10)
β, deg	98.3917(12)	98.1230(10)
γ, deg		92.8550(10)
V, Å^3	3031.6(3)	553.25(6)
Z	8	2
ρ(calcd), Mg m^{-3}	1.56	1.94
radiation (λ, Å)	Mo Kα (0.71073)	Mo Kα (0.71073)
abs coeff μ, mm^{-1}	0.691	0.981
θ range for data collection (deg)	1.76−28.31	1.76−28.27
reflns collected	19630	3747
indep reflns	7332	2570
R1 ($[I > 2\sigma(I)]$)[a]	0.0808	0.0387
wR2 (all data)[a]	0.1563	0.1057
abs corr	SADABS	SADABS
transm factors	0.691−0.962	0.601−0.983

[a] $R1 = \sum||F_o| - |F_c||/\sum|F_o|$; $wR2 = \{\sum[w(F_o^2 - F_c^2)^2]/\sum[w(F_o^2)^2]\}^{1/2}$.

(m), 1227 (w), 1165 (vw), 1127 (m), 1095 (w), 1070 (s), 1028 (w), 947 (vs, V═O), 940 (vs, V═O), 882 (s), 817 (m), 804 (s), 758 (s), 723 (w), 577 (m), 559 (m), 448 (m). ^{1}H NMR (D_2O, ppm, DSS): 7.150 (py-*H*, 6H), 3.168 ($N(CH_3)_4^+$, 60H) (297 K, pH 4.71). ^{1}H NMR (D_2O, ppm, DSS): 7.520 (py-*H*, 6H), 3.160+3.157 ($N(CH_3)_4^+$, 60H) (297 K, pH 3.29). ^{51}V NMR (D_2O, ppm, $VOCl_3$): −524.0 (99.4%, complex), −560.7 (0.6%, V_1) (297 K, pH 4.71). −528.6 (297 K, pH 3.29). Calcd for $C_{41}H_{75}N_8O_{25}V_3$: C 39.94, H 6.09, N 9.09. Found: C 39.85, H 6.04, N 8.99.

Crystallographic Studies on $Na[VO_2(dipic\text{-}OH)]\cdot 2H_2O$ and $(NMe_4)[VO_2(dipic\text{-}OH)]\cdot H_2O$. X-ray diffraction data from colorless crystals with dimensions of 0.35 × 0.23 × 0.10 mm ($Na[VO_2(dipic\text{-}OH)]\cdot 2H_2O$) and 0.36 × 0.15 × 0.06 mm {$(NMe_4)[VO_2(dipic\text{-}OH)]\cdot H_2O$} were recorded on a Bruker AXS SMART CCD diffractometer employing Mo Kα radiation. Crystallographic results and other details are listed in Table 1. The cell parameters were obtained from a least-squares fit to the angular coordinates of all reflections for both compounds. Intensities were integrated from a series of frames (0.3° ω rotation) covering more than a hemisphere of reciprocal space. Absorption and other corrections were applied by using SADABS.[26] The structures were solved by using direct methods {$Na[VO_2(dipic\text{-}OH)]\cdot 2H_2O$} or Patterson superposition methods {$(NMe_4)[VO_2(dipic\text{-}OH)]\cdot H_2O$} and refined (on F^2, all data) by a weighted full-matrix least-squares process. All nonhydrogen atoms were refined by using anisotropic atomic displacement parameters. Hydrogen atoms were located in an electron density map and refined with isotropic displacement parameters except for those of the tetramethylammonium cations in $(NMe_4)[VO_2(dipic\text{-}OH)]\cdot H_2O$, in which the hydrogen atoms were placed in idealized positions and refined by using a rotating riding model. The final electron density map showed features in the range from −0.64 to +0.46 e Å^{-3} for $Na[VO_2(dipic\text{-}OH)]\cdot 2H_2O$ and from −0.46 to +0.46 e Å^{-3} for $(NMe_4)[VO_2(dipic\text{-}OH)]\cdot H_2O$. Standard Bruker control (SMART) and integration (SAINT) software was employed, and Bruker SHELXTL[27] software was used for structure solution, refinement, and graphics.

Sample Preparation for Solution Studies. Samples for spectroscopic analyses in solution were prepared by several methods. In one method, ligand was added to deuterium oxide and partially dissolved before addition of NH_4VO_3. Alternatively, the two solids were added to D_2O at the same time, but then the solution needs to be heated to convert the initially formed orange decavanadate to vanadate, which can then form the complex. Finally, ligand and NH_4VO_3 were dissolved separately in deuterium oxide and the solutions then combined. When necessary, the pH was adjusted with a stock solution of DCl or NaOD. Samples for ^{13}C NMR also contained 33% (v/v) deuterium oxide. Samples for ^{17}O NMR were prepared by dissolving the solid complex and were enriched with $[^{17}O]H_2O$ to 2−4 atom % $[^{17}O]H_2O$. The pH values of solution were measured by a pH meter and were not adjusted for the presence of D_2O.

1D NMR Spectroscopy. The 1D ^{1}H, ^{51}V, and ^{17}O spectra were recorded on a Varian INOVA-300 spectrometer (7.0 T) at 300 MHz for ^{1}H, 78.9 MHz for ^{51}V, and 40.7 MHz for ^{17}O. 1D ^{13}C spectra were recorded on a Varian INOVA-400 spectrometer (9.4 T) at 100.6 MHz for ^{13}C. Routine parameters were used for the 1D ^{1}H NMR experiments. The ^{13}C spectra were acquired with a 25000 Hz spectral window, a 90° pulse width, an acquisition time of 0.632 s, and a relaxation delay of 1.3 s. A 5 Hz exponential line broadening was applied prior to Fourier transformation. An external reference of sodium 3-(trimethylsilyl)propanesulfonate (DSS) was used for ^{1}H and ^{13}C chemical shifts. ^{51}V NMR spectra were acquired with a spectral window of 83600 Hz, a pulse angle of 60°, and an acquisition time of 0.096 s with no relaxation delay. ^{51}V NMR chemical shifts were referenced against an external sample of $VOCl_3$. A 15 Hz exponential line broadening was applied before Fourier transformation. The mole fractions of complex and other vanadium(V) compounds were measured by using Varian integration software. Assuming that all vanadium present in solution was in the form of vanadium(V) and that all species had similar relaxation times, concentrations of complex and oligomeric oxovanadates could be derived. The ^{17}O NMR spectra were recorded with a spectral window of 80000 Hz, a pulse angle of 90°, and an acquisition time of 0.05 s with no relaxation delay. Water was used as an internal reference for ^{17}O NMR chemical shifts.

Variable-temperature ^{13}C NMR spectra were also recorded. The temperature for the variable-temperature experiments was calibrated to an accuracy of ±2° by using an 80% ethylene glycol sample in DMSO-d_6.[24] Spectra were recorded first at 298 K and then at higher temperatures. The sample was equilibrated for 10 min at each temperature before the spectrum was recorded. At the end of the temperature series, the sample was cooled back to 298 K and the spectrum rerecorded to ensure that no changes in the sample had taken place during the variable-temperature experiment.

2D EXSY NMR Spectroscopy. The 2D ^{1}H EXSY experiments were run on a Varian INOVA-300 spectrometer (7.0 T) at 300 MHz for ^{1}H at 297 K; the ^{13}C EXSY experiments were run on a Varian INOVA-400 spectrometer (9.4 T) at 100.6 MHz for ^{13}C at 298 and 308 K. The 2D ^{1}H EXSY spectra were recorded with a width of 459 Hz, an accumulation time of 0.139 s, a delay time of 3.0 s, a mixing time of 0.5 s, and 128 increments of 4 scans each. The 2D ^{13}C EXSY spectra were recorded with a width of 8870 Hz, an accumulation time of 0.231 s, a delay time of 2.0 s, a mixing time of 0.5 s, and 128 increments of 8 scans each. The signal region of

(26) Sheldrick, G. M. *SADABS (a Program for Siemens Area Detection Absorption Correction)*; University of Göttingen: Göttingen, Germany, 2000.

(27) Sheldrick, G. M. *SHELXTL*, version 5; Bruker-Nonius: Madison, WI, 1996.

interest included only the spectral window of interest in order to increase sensitivity. This reduced the size of the data matrix required in the F1 domain and decreased accumulation times. Shorter mixing times were also used, but the observed cross signals were smaller, and accordingly the spectra were of poorer quality and are not shown herein.

Results and Discussion

Syntheses. As described above, the chelidamic acid complex of V(V) can be synthesized from sodium metavanadate ($NaVO_3$) and ligand. Since the pK_a value of the hydroxyl group of chelidamic acid decreases upon complex formation,[9,28] more than one complex should form (with $[dipic\text{-}OH]^{2-}$ at lower pH and with $[dipic\text{-}O^{-}]^{3-}$ at higher pH). At pH values close to the ligand's third pK_a value, the hydroxyl group is partially deprotonated and either form of the ligand may be bound to the metal.[29] The reaction between $NaVO_3$ and chelidamic acid at pH 1.1 generated the $[VO_2(dipic\text{-}OH)]^{-}$ complex only. Attempts to prepare the complex involving the fully deprotonated ligand, $[VO_2(dipic\text{-}O^{-})]^{2-}$, were unsuccessful, in that the resulting material contained some vanadate (10% V_i by ^{51}V NMR) or free ligand (30% by ^{1}H NMR).

More information on the solid state properties of the chelidamate complex was desired, and a second compound, $[NMe_4][VO_2(dipic\text{-}OH)]$, was obtained with the more hydrophobic tetramethylammonium cation as the counterion. As described above, the tetramethylammonium salt was prepared by reaction of V_2O_5 with neutral ligand at pH 4.3 by using aqueous tetramethylammonium hydroxide to adjust the pH. Crystalline $[NMe_4][VO_2(dipic\text{-}OH)]$ was obtained from the initial reaction solution, and a second compound formulated as $(NMe_4)_5\{[VO_2(dipic\text{-}OH)][VO_2(dipic\text{-}O^{-})]_2\}\cdot 4H_2O$ was isolated later. This compound, which contained the ligand in two protonation states, is similar to another recently reported compound.[29]

Structure of $NMe_4[VO_2(dipic\text{-}OH)]\cdot H_2O$. The $(NMe_4)[VO_2(dipic\text{-}OH)]\cdot H_2O$ compound contains discrete $[VO_2(dipic\text{-}OH)]^{-}$ complex anions. The structure of the complex is shown in Figure 1; a diagram representing the packing in the solid state is shown in Figure 2. Selected interatomic distances, angles, and hydrogen bond distances are given in Table 2. The asymmetric unit contains two formula units of $(NMe_4)[VO_2(dipic\text{-}OH)]\cdot H_2O$, which exhibit only minor structural differences. The vanadium(V) atom is five-coordinate by virtue of coordination by two oxo ligands and the tridentate $[dipic\text{-}OH]^{2-}$ ligand (utilizing two carboxylate oxygen atoms and the pyridine nitrogen atom). The hydroxyl group (O(5), O(15)), one carboxylate oxygen atom (O(3), O(13)), and one oxo ligand (O(6), O(16)) from each of the $[VO_2(dipic\text{-}OH)]^{-}$ ions in the asymmetric unit form hydrogen bonds to water molecules (see Table 3), resulting in extended chains of $[VO_2(dipic\text{-}OH)]^{-}$ anions. The chains are separated by the tetramethylammonium cations.

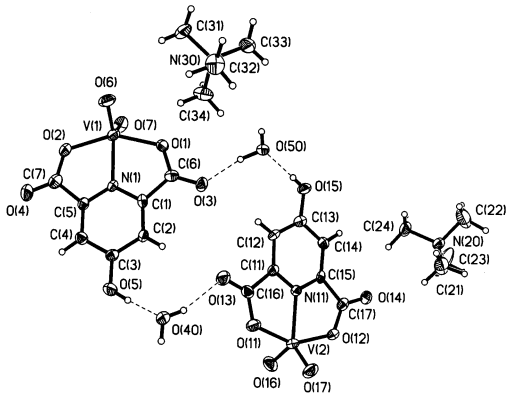

Figure 1. Structure of the contents of an asymmetric unit for $(NMe_4)[VO_2(dipic\text{-}OH)]\cdot H_2O$, with 50% probability thermal ellipsoids for nonhydrogen atoms. Hydrogen atoms are shown as spheres of arbitrary radius.

Table 2. Selected Bond Lengths and Angles for $NMe_4[VO_2(dipic\text{-}OH)]\cdot H_2O$

Bond Lengths (Å) and Angles (deg)			
V(1)−O(7)	1.615(3)	V(11)−O(17)	1.612(3)
V(1)−O(6)	1.626(3)	V(11)−O(16)	1.627(3)
V(1)−O(2)	1.998(4)	V(11)−O(12)	1.997(3)
V(1)−O(1)	2.022(3)	V(11)−O(11)	2.026(3)
V(1)−N (1)	2.077(4)	V(11)−N(11)	2.070(4)
O(1)−C(6)	1.286(5)	O(11)−C(16)	1.293(6)
O(2)−C(7)	1.296(6)	O(12)−C(17)	1.299(6)
O(3)−C(6)	1.236(6)	O(13)−C(16)	1.229(6)
O(4)−C(7)	1.225(6)	O(14)−C(17)	1.219(6)
O(7)−V(1)−O(6)	110.69(19)	O(17)−V(11)−O(16)	110.93(19)
O(7)−V(1)−O(2)	99.29(17)	O(17)−V(11)−O(12)	98.94(17)
O(6)−V(1)−O(2)	99.26(17)	O(16)−V(11)−O(12)	99.31(16)
O(7)−V(1)−O(1)	98.45(16)	O(17)−V(11)−O(11)	99.06(17)
O(6)−V(1)−O(1)	98.10(16)	O(16)−V(11)−O(11)	97.28(16)
O(2)−V(1)−O(1)	148.88(14)	O(12)−V(11)−O(11)	149.22(14)
O(7)−V(1)−N(1)	123.37(17)	O(17)−V(11)−N(11)	120.67(18)
O(6)−V(1)−N(1)	125.92(18)	O(16)−V(11)−N(11)	128.39(18)
O(2)−V(1)−N(1)	74.41(14)	O(12)−V(11)−N(11)	74.82(14)
O(1)−V(1)−N(1)	74.48(14)	O(11)−V(11)−N(11)	74.55(15)

Hydrogen Bonds (Å) (D = Donor Atom, A = Acceptor Atom) and D−H−A Angles (deg)

D−H···A	D−H	H···A	D···A	D−H−A
O(15)−H(15A)···O(40)	0.69(4)	1.87(4)	2.549(5)	172(5)
O(40)−H(40B)···O(3)	0.93(6)	1.81(6)	2.726(5)	168(5)
O(50)−H(50A)···O(6)	0.84(6)	1.90(6)	2.737(6)	179(6)
O(5)−H(5A)···O(50)#1[a]	0.85(6)	1.71(6)	2.565(6)	174(6)
O(40)−H(40A)···O(16)#2	0.77(5)	1.96(5)	2.727(5)	174(5)
O(50)−H(50B)···O(13)#2	0.81(8)	1.95(8)	2.720(6)	158(7)

[a] Symmetry transformations used to generate equivalent atoms: #1 = $x - 1, y, z$; #2 = $x + 1, y, z$.

The oxo ligands (O(6), O(16)) that are involved in hydrogen bonding with water form slightly longer bonds to vanadium (1.626(3), 1.627(3) Å) than do the oxo ligands (O(7), O(17)) that do not participate in hydrogen bonding (1.615(3), 1.612(3) Å). The shorter V═O bond lengths are similar to the V═O bond lengths observed in $[VO_2(dipic)]^{-}$ (1.610(6), 1.615(6) Å).[30] Hydrogen bonding to water does not seem to influence significantly the C−O(carboxylate) bond lengths. Other bond lengths and angles in the primary coordination sphere (V−O(carboxylate), V−N(pyridine), and V−O(oxo)) are similar to those observed for $[VO_2(dipic)]^{-}$.[30]

(28) Pike, M. M.; Yarmush, D. M.; Balschi, J. A.; Lenkinski, R. E.; Springer, C. S., Jr. *Inorg. Chem.* **1983**, *22*, 2388−2392.
(29) Hall, A. K.; Harrofield, J. M.; Skelton, B. W.; White, A. H. *Acta Crystallogr.* **2000**, *C56*, 407−411.
(30) Nuber, B.; Weiss, J.; Wieghardt, K. *Z. Naturforsch.* **1978**, *33B*, 265−267.

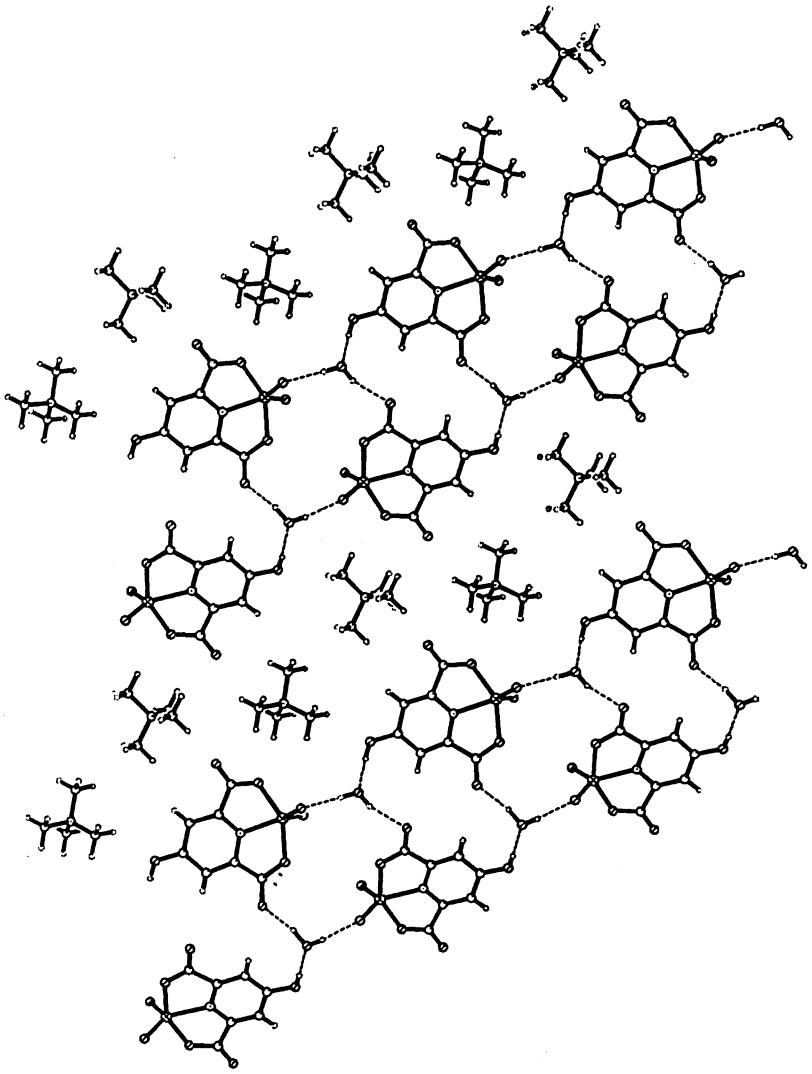

Figure 2. Packing diagram for $(NMe_4)[VO_2(dipic\text{-}OH)]\cdot H_2O$, showing the chains of complex anions linked together by hydrogen bonding and separated by a belt of discrete counterions.

An asymmetry in the V−O(carboxylate) bonding is observed; V−O(2) (1.998(4) Å) is slightly shorter than V−O(1) (2.022(3) Å), and a corresponding asymmetry is also observed for the other complex ion in the asymmetric unit.

Structure of $Na[VO_2(dipic\text{-}OH)]\cdot 2H_2O$. The structure of the complex is shown in Figure 3; a diagram representing the packing in the solid state is shown in Figure 4. Selected interatomic distances, angles, and hydrogen bond distances are given in Table 3. The asymmetric unit contains two formula units of $Na[VO_2(dipic\text{-}OH)]\cdot 2H_2O$. As in $(NMe_4)[VO_2(dipic\text{-}OH)]\cdot H_2O$, the vanadium(V) atom is five-coordinate by virtue of coordination to two oxo ligands and the tridentate $[dipic\text{-}OH]^{2-}$ ligand.

The Na^+ cation is incorporated into a polymeric chain formed by coordination of Na^+ by $[VO_2(dipic\text{-}OH)]^-$ anions. The sodium ion is six-coordinate by virtue of coordination to two water molecules (O(8), O(9)), to two bridging oxo ligands (from two symmetry-related complexes (O(7), O(7B) in Figure 3), and to two carboxylate oxygen atoms from a third symmetry-related complex (O(2A), O(4A) in Figure 3). The carboxylate group at C(7) is therefore in a μ^3 coordination mode, and the group at C(6) is in a terminal monodentate coordination mode. The hydroxyl group O(5) (H-donor), the carboxylate group at C(6) (H-acceptor), and the oxo ligand O(6) (H-acceptor) form hydrogen bonds to the water molecules coordinated to the sodium ion, resulting in a linking together of the polymeric chains into extended sheets (Figure 4).

Hydrogen bonding to water and coordination to the sodium ion influences bond lengths within the carboxylate groups. For example, the difference in the C−O bond lengths in the carboxylate at C(6) (1.295(3), 1.233(3) Å), which engages in hydrogen bonding to water through O(3), is less pronounced than the difference in the C−O bond lengths seen in the carboxylate at C(7) (1.305(3), 1.223(3) Å), where both of the oxygen atoms coordinate the sodium ion. In contrast, for the oxo ligands hydrogen bonding to water (O(6)) or coordination to sodium (O(7)) does not result in an observable difference between the V═O distances (V═O(6), 1.626(2) Å; V═O(7), 1.629(2) Å). These distances are similar to the V═O distances in $(NMe_4)[VO_2(dipic\text{-}OH)]\cdot H_2O$ (1.6264(17), 1.6290(17) Å) and slightly longer than those observed in the parent compound $Cs[VO_2(dipic)]\cdot H_2O$ (1.610(6)/1.615(6) Å).[30] Otherwise bond distances and angles

Table 3. Selected Bond Lengths and Angles for $Na[VO_2(dipic\text{-}OH)]\cdot 2H_2O$

Bond Lengths (Å) and Angles (deg)			
V−O(7)	1.6264(17)	Na−O(9)	2.461(2)
V−O(6)	1.6290(17)	Na−O(4)#2[a]	2.4827(19)
V−O(2)	1.9945(16)	Na−O(2)#2	2.5745(18)
V−O(1)	2.0011(16)	Na−C(7)#2	2.853(2)
V−N(1)	2.0770(19)	Na−Na#1	3.7454(19)
V−Na	3.5161 (11)	O(2)−C(7)	1.305(3)
Na−O(8)	2.278(2)	O(1)−C(6)	1.295(3)
Na−O(7)#1	2.3973(19)	O(3)−C(6)	1.233(3)
Na−O(7)	2.4390(19)	O(4)−C(7)	1.223(3)

O(7)−V−O(6)	109.78(9)	O(8)−Na−O(9)	83.93(8)
O(7)−V−O(2)	100.01(8)	O(7)#1−Na−O(9)	169.72(8)
O(6)−V−O(2)	98.58(8)	O(7)−Na−O(9)	109.51(7)
O(7)−V−O(1)	98.43(8)	O(8)−Na−O(4)#2	130.54(8)
O(6)−V−O(1)	97.86(8)	O(7)#1−Na−O(4)#2	94.45(7)
O(2)−V−O(1)	149.42(7)	O(7)−Na−O(4)#2	137.71(7)
O(7)−V−N(1)	125.71(8)	O(9)−Na−O(4)42	83.87(6)
O(6)−V−N(1)	124.48(8)	O(8)−Na−O(2)42	171.65(8)
O(2)−V−N(1)	74.96(7)	O(7)#1−Na−O(2)#2	98.18(6)
O(1)−V−N(1)	74.47(7)	O(7)−Na−O(2)#2	87.10(6)
O(8)−Na−O(7)#1	89.55(8)	O(9)−Na−O(2)#2	88.84(6)
O(8)−Na−O(7)	91.39(7)	O(4)#2−Na−O(2)#2	52.30(5)
O(7)#1−Na−O(7)	78.49(7)		

Hydrogen Bond Lengths (Å) (D = Donor, A = Acceptor) and D−H−A Angles (deg)

D−H···A	D−H	H···A	D···A	D−H···A
O(9)−H(9A)···O(6)	0.91(5)	2.33(5)	3.062(2)	138(4)
O(5)−H(5A)···O(9)#3	0.82(4)	1.82(4)	2.634(2)	169(4)
O(8)−H(8A)···O(1)#4	0.83(6)	2.13(6)	2.945(3)	166(5)
O(8)−H(8B)···O(6)#5	0.75(4)	2.20(4)	2.923(3)	163(4)
O(9)−H(9A)···O(6)#6	0.91(5)	2.23(5)	3.004(3)	143(4)
O(9)−H(9B)···O(3)#4	0.78(4)	2.01(4)	2.744(3)	157(3)

[a] Symmetry transformations used to generate equivalent atoms: #1 = $-x, -y+1, -z$; #2 = $-x+1, -y+1, -z$; #3 = $x, y, z+1$; #4 = $-x, -y+2, -z$; #5 = $x-1, y, z$; #6 = $-x+1, -y+2, -z$.

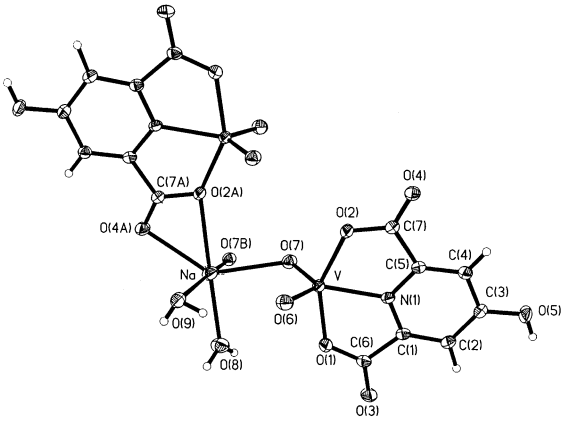

Figure 3. Structure of $Na[VO_2(dipic\text{-}OH)]\cdot H_2O$, with 50% probability thermal ellipsoids for non-hydrogen atoms. Two complex anions, $[VO_2(dipic\text{-}OH)]^-$, are shown linked together by six-coordinate Na^+.

in the coordination sphere of the V(V) atom in $Na[VO_2(dipic\text{-}OH)]\cdot 2H_2O$ are similar to the corresponding parameters in $(NMe_4)[VO_2(dipic\text{-}OH)]\cdot H_2O$ and $Cs[VO_2(dipic)]\cdot H_2O$.[30] The most significant difference among these structures arises from the formation of a polymeric structure as a result of the interactions of the sodium ion with coordinated dipic-OH^{2-} ligands.

IR Spectroscopy. The IR spectra (KBr pellet) of $(NMe_4)[VO_2(dipic\text{-}OH)]\cdot H_2O$ and $Na[VO_2(dipic\text{-}OH)]\cdot 2H_2O$ are similar. The $\nu_{as}(CO_2^-)$ and $\nu_s(CO_2^-)$ bands at 1681 (1681) cm^{-1} and 1379 (1380) cm^{-1}, respectively, are both strongly absorbing, as are the V═O stretching vibrations (948 (945) cm^{-1}). Although two stretching vibrations should be observable in the IR for V═O, the single peak reported is very broad with a shape suggestive of a shoulder, which we have not attempted to deconvolute. The peak in the vicinity of 1055 cm^{-1} is assigned to the C−O(hydroxy) vibration. The OH stretching vibration of water molecules/py-OH in the sodium salt is at higher energy (3474 cm^{-1}) than in the tetramethylammonium salt (3434 cm^{-1}), indicating that the hydrogen bonds are stronger in the case of the tetramethylammonium salt. Hydrogen bonds are also represented by several weak absorptions in the 2480−2750 cm^{-1} region, and again the peaks for the sodium salt occur at higher energies than for the tetramethylammonium salt.

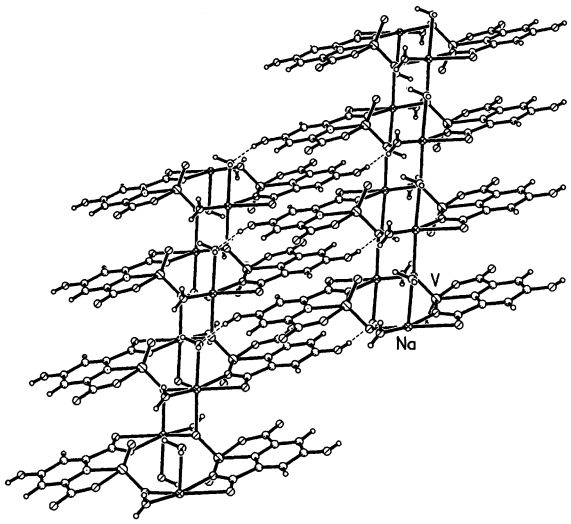

Figure 4. Packing diagram for $Na[VO_2(dipic\text{-}OH)]\cdot 2H_2O$. Polymeric chains formed by the complex anion $[VO_2(dipic\text{-}OH)]^-$ and the six-coordinate Na^+ counterion are shown. The chains are linked together by hydrogen bonding.

The $\nu_{as}(CO_2^-)$ in the compound $(NMe_4)_5\{[VO_2(dipic\text{-}OH)][VO_2(dipic\text{-}O^-)]_2\}\cdot 4H_2O$ occurs at a lower energy (1643 cm^{-1}) and $\nu_s(CO_2^-)$ at a higher energy (1388 cm^{-1}) compared to the sodium and tetramethylammonium compounds above. Two strong V═O stretching vibrations are seen at 947 and 940 cm^{-1}, and the C−O(hydroxyl) absorption appears around 1070 cm^{-1}. These peaks indicate that this compound may not be a simple mixture involving protonated and deprotonated ligands. The peaks at 3559 and 3325 cm^{-1} are attributed to OH vibrations; the latter is a sharp peak. Several new peaks (at 1524, 1512, 882, 817, 559 cm^{-1}) support the conclusion that this is a new and different compound.

Speciation, Formation Constants, and pK_a Values. Spectroscopic studies were conducted to characterize the stability of the complex as a function of pH and to determine the stoichiometry of the species forming in aqueous solution. ^{51}V NMR spectra showed only one pH-dependent signal for solutions of $Na[VO_2(dipic\text{-}OH)]$ and $(NH_4)[VO_2(dipic\text{-}OH)]$[31] in the pH range 1.5−6. The same spectra were obtained by using (a) stock solutions of vanadate salts and

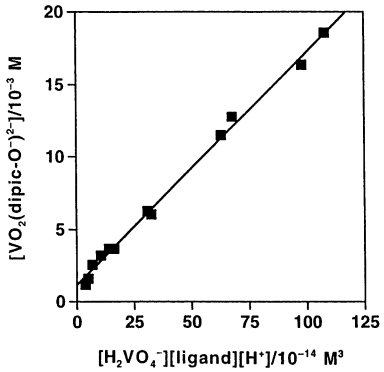

Figure 5. Plot of $[VO_2(dipic\text{-}O^-)^{2-}]$ as a function of $[ligand][H_2VO_4^-][H^+]$. The solutions used to obtain these curves contained 4.0−20.1 mM vanadate and 6.4−31.9 chelidamic acid.

H_2dipic-OH ligand or (b) the crystalline compounds, which demonstrates that the complex ion is formed rapidly in this pH range. At pH values of 6.7 and above, less of the complex exists and signals for oligovanadates (^{51}V NMR) and ligand (^{1}H NMR) indicate that the complex hydrolyzes.

The stoichiometry of the complex was determined from ^{1}H and ^{51}V NMR spectra of solutions containing from 40.0 mM vanadate salt/69.0 mM H_2dipic-OH to 4.0 mM vanadate salt/6.4 mM H_2dipic-OH. None of the solutions contained added salts. Given the low charge and high stability of the complex, the modest change in ionic strength in these solutions should not significantly affect the measurements, although high ionic strength decreases complex formation[32] and the values obtained in this study will be slightly higher than those that would be observed at higher ionic strength. As reflected in eq 1, a linear relationship is expected between $[(VO_2(dipic\text{-}O^-))^{2-}]$ and $[H_2VO_4^-][dipic\text{-}OH^{2-}{}_{free}][H^+]$ for a 1:1 complex; such a linear relationship was observed (see Figure 5). A linear relationship was not observed when $[(VO_2(dipic\text{-}O^-))^{2-}]$ was plotted vs expressions derived for complexes of other stoichiometries. These data are consistent with the complex observed at −522 or at −530 ppm in the ^{51}V NMR spectrum having a 1:1 stoichiometry.

In a plot of [complex] and the ratio [complex]/[V_1] as a function of pH, the stability of the complex can be illustrated regardless of the forms of the vanadium(V). Here [V_1] represents the total observed mononuclear vanadium(V), which corresponds to the sum of $[VO_4^{3-}] + [H_2VO_4^-] + [HVO_4^{2-}] + [VO_2^+]$. Although [complex] changes smoothly, the [complex]/[V_1] ratio gives a bell curve with a maximum at a pH of ∼3.5, where the ratio is much higher than at any other pH. The high maximum in [complex]/[V_1] ratio is attributed to the low concentration of [V_1] at this pH. The complex formed in the pH range 6.6−7.9 is described in reaction 1; the equilibrium constant for that reaction was 1.6 (±0.1) × 10^{10} M^{-2}. Measurements were also carried out in acidic solution at pH 0.3−0.7, under conditions where the vanadium(V) is in the form of VO_2^+. Under these conditions, the complex formation reaction may be described as shown

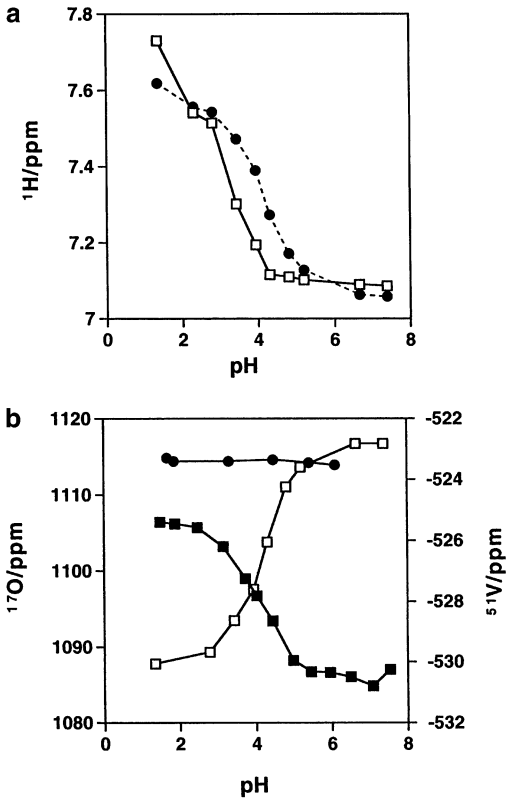

Figure 6. ^{51}V, ^{1}H, and ^{17}O chemical shifts of complex and ^{1}H chemical shifts of ligand are plotted as functions of pH. The ^{1}H (Figure 6a: solid circles for complex and open squares for free ligand) and ^{51}V (Figure 6b: open squares) spectral data shown were obtained from solutions of 40 mM NH_4VO_3 and 69 mM H_2dipic-OH. The ^{17}O NMR spectra were obtained by adding 224 mM crystalline complex into 10% ^{17}O-H_2O (Figure 6b: solid squares for $[VO_2(dipic\text{-}OH)]^-$, solid circles for $[VO_2(dipic)]^-$).

in eq 2; and the equilibrium constant for this reaction was 92 (±7) M^{-1}.

$$H_2VO_4^- + dipic\text{-}OH^{2-} + H^+ \rightleftarrows [VO_2(dipic\text{-}O^-)]^{2-} + 2H_2O \quad (1)$$

$$VO_2^+ + H_2dipic\text{-}OH \rightleftarrows [VO_2(dipic\text{-}OH)]^- + 2H^+ \quad (2)$$

The ^{51}V chemical shift for the dianion is −522 ppm (above pH 6) and for the monoanion −530 ppm (below pH 3). Figure 6 shows a plot of the ^{1}H chemical shifts as a function of pH, both for the complex and for the free ligand (the two aromatic protons in the complex give only one pH-dependent chemical shift). From the changes in the ^{1}H chemical shift values, the pK_a of the complex can be calculated to be 4.1 (±0.1) by using eq 3.[33] In eq 3, δ_L represents the minimum chemical shift, δ_H the maximum chemical shift, and δ_O the chemical shift at intermediate pH values. The signal for free ligand is also pH-dependent, and the analysis gives three pK_a values at 1.4 (±0.2), 3.4 (±0.2), and 11.6 (±0.3). These values correspond well to those from potentiometric methods (<2, 3.47 (±0.01), 11.4).[9] The pK_a of the complex was found to be 4.1 (±0.2) by ^{51}V NMR spectroscopy and 4.1 (±0.1) by ^{17}O NMR spectroscopy. Excellent agreement is observed between the pK_a value measured by three different techniques

(31) Studies were carried out with both sodium and ammonium salts. The results from these parallel speciation studies were indistinguishable.
(32) Crans, D. C. *Comments Inorg. Chem.* **1994**, *16*, 1−33.
(33) Jaswal, J. S.; Tracey, A. S. *Can. J. Chem.* **1991**, *69*, 1600−1607.

and the results obtained from solutions of (a) mixtures of vanadate and ligand (^{1}H and ^{51}V) and (b) crystalline complex (^{17}O).

$$pH = pK_a + \log[(\delta_L - \delta_O)/(\delta_O - \delta_H)] \quad (3)$$

Solution Structure of the $[VO_2(dipic\text{-}OH)]^-$ Anion. ^{1}H, ^{13}C, and ^{17}O NMR spectra were recorded to obtain information on the solution structure of the complex. For spectral characterization of signals the numbering system for the first complex anion in Figure 1 was used (C1−C7). Only two protons (H2/H4) on the aromatic ring could be observed by ^{1}H NMR spectroscopy. The signal for these two protons is significantly shifted from that for the corresponding protons of the uncomplexed ligand; at pH 3.9 the complex and ligand protons were observed at 7.39 and 7.19 ppm, respectively. In the ^{13}C NMR spectrum at pH 3.6 the chemical shifts of all of the carbon atoms were affected by complexation: (a) the carboxylate carbon atoms (C6/C7 179.4 ppm, L6/L7 183.9 ppm); (b) the carbon atoms ortho to the pyridine nitrogen atom (C1/C5 173, L1/L5 168 ppm); (c) the meta carbon atoms (C2/C4 117.5, L2/L4 118.9); and (d) the para carbon atom (C3 152 ppm, L3 147 ppm). These assignments were consistent with the slow relaxation times for the carboxyl and ternary carbon atoms and the inductive and resonance effects expected for a heteroaromatic ring system coordinated in a tridentate manner to vanadium. A DEPT experiment supported this interpretation.

The ^{1}H, ^{13}C, ^{17}O, and ^{51}V chemical shifts for complex and/or free ligand were observed as a function of pH (see Figure 6). Above pH 4 the ^{1}H NMR chemical shift for uncomplexed ligand changed little. However, large changes were observed by ^{13}C NMR spectroscopy on deprotonation of the complex. Deprotonation of the complex induced a change in the chemical shift for C6/C7 in the complex of more than 5 ppm, while the chemical shifts for C2/C4 and C3 changed by ∼2−3 ppm. Monitoring the titration of the complex by base by using ^{51}V NMR spectroscopy confirmed that the deprotonation of the hydroxyl substituent of $[VO_2(dipic\text{-}OH)]^-$ took place at about pH 4. Deprotonation of this same hydroxyl substituent in the uncomplexed ligand takes place at about pH 11 (data not shown and ref 9). Below pH 2 the chemical shifts for the uncomplexed ligand changed due to protonation of the pyridine nitrogen atom.[34] The stability of the complex is decreased below pH 1, and the ^{51}V chemical shift for the complex in this pH range continues to change, presumably due to complex protonation.

^{17}O NMR data were obtained to gain information on the coordination of oxygen. Two possible five-coordinate $[VO_2(dipic\text{-}OH)]^-$ complexes can be considered, one with a cis arrangement of the oxo ligands and one with a trans arrangement. Both arrangements would yield a ^{17}O signal at about 1000 ppm. The possible cis and trans six-coordinate complexes would have more than one ^{17}O signal at about 1000 ppm, assuming that a potential sixth ligand (presumably H_2O) did not exchange rapidly with solvent water. Like the parent complex, $[VO_2(dipic\text{-}OH)]^-$ gives only one broad signal at 1095 ± 10 ppm (depending on pH) by ^{17}O NMR spectroscopy. Variable-temperature studies showed that the broad signal did not sharpen at higher temperature nor did it broaden or split into two signals at lower temperatures. We conclude that the solution structures of $[VO_2(dipic\text{-}OH)]^-$ and $[VO_2(dipic)]^-$ are very similar.[25]

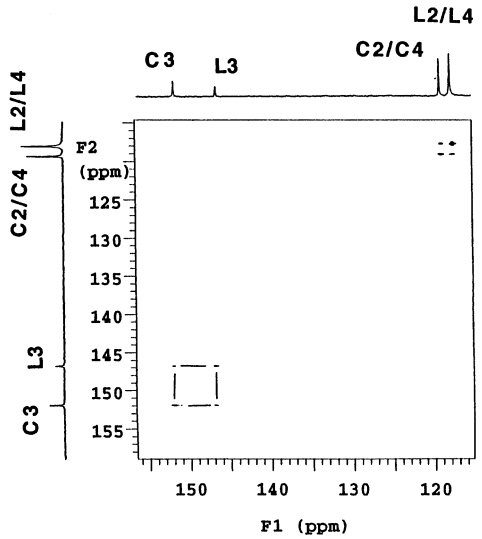

Figure 7. ^{13}C EXSY spectrum (partial) of solution containing 515 mM NH_4VO_3 and 836 mM ligand H_2dipic-OH at pH 3.6 (±0.1).

Motional Processes and Lability of the $[VO_2(dipic\text{-}OH)]^-$ Anion. Variable-temperature ^{1}H, ^{51}V, and ^{13}C NMR spectra were recorded for solutions prepared by three different methods. One set of solutions was prepared by dissolving the crystalline solid containing the $[VO_2(dipic\text{-}OH)]^-$ complex, a second set of solutions was prepared by dissolving crystalline solid and excess ligand, and a third set of solutions contained NH_4VO_3 and ligand. Dynamic processes were observed for all pH values examined. For example, the variable-temperature ^{13}C NMR spectra (298−328 K) of a solution containing 515 mM NH_4VO_3 and 836 mM H_2dipic-OH at pH 3.6 showed broadening of all ^{13}C signals as the temperature was increased (data not shown). In contrast, in the corresponding experiment at pH 6.7 the exchange broadening was decreased below detection (data not shown). No decomposition reactions took place, as in each case an identical spectrum was obtained after completing the variable-temperature experiment and returning to the initial temperature. To obtain additional information regarding the nature of the dynamic process, homonuclear ^{1}H and ^{13}C EXSY NMR spectra were recorded.

EXSY Spectroscopy. ^{1}H and ^{13}C NMR EXSY spectroscopy was used to determine how the pH affects intermolecular processes such as ligand exchange in solutions containing $[VO_2(dipic\text{-}OH)]^-$. The ^{13}C EXSY NMR spectrum of a sample containing NH_4VO_3 (515 mM) and free ligand (836 mM) at pH 3.6 (±0.1) is shown in Figure 7. The corresponding ^{1}H EXSY NMR spectrum is shown in Figure 8 for a solution of 40.1 mM NH_4VO_3 and 69.3 mM free complex at pH 3.5 (±0.1). Solid lines in Figure 7 indicate the cross-peaks between C3 of the complex and C3 of the ligand. Solid lines in Figure 8 indicate the cross peaks

(34) Hall, A. K.; Harrofield, J. M.; Skelton, B. W.; White, A. H. *Acta Crystallogr.* **2000**, *C56*, 448−450.

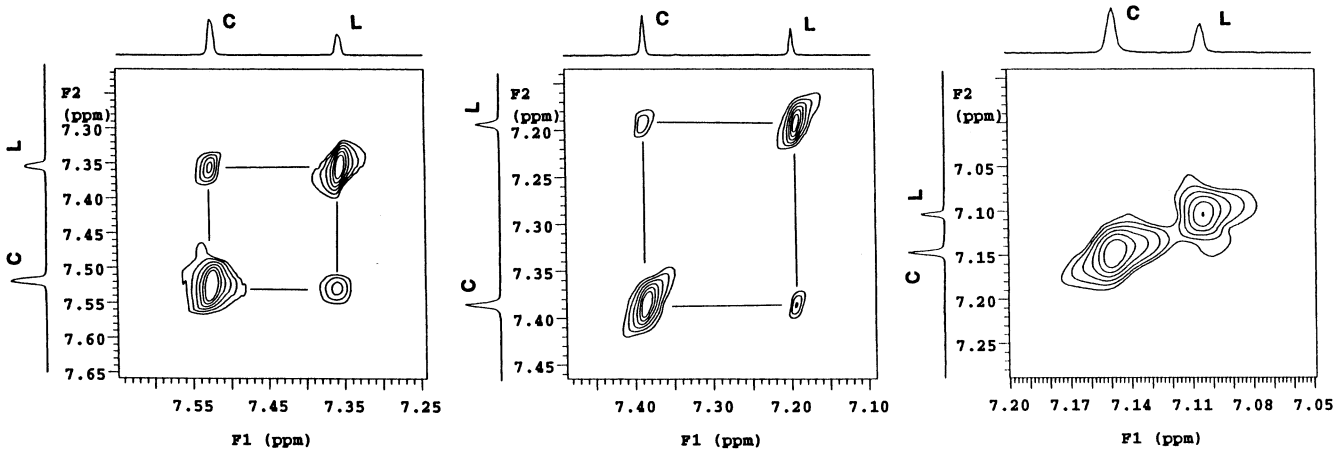

Figure 8. ^{1}H EXSY spectra of solutions containing 40 mM NH_4VO_3 and 69 mM H_2dipic-OH at pH 3.5 (±0.1) (left), 3.7 (±0.1) (center), and 5.0 (±0.1) (right).

between H2 of the complex and H2 of the ligand. These cross signals establish that the dipic-OH^{2-} in the $[VO_2(\text{dipic-OH})]^-$ anion is exchanging with dipic-OH^{2-} in solution on the time scale of the ^{1}H and ^{13}C NMR experiments.

The ^{1}H NMR EXSY spectra were recorded at pH values of 3.1, 3.5, 3.7, 3.9, 4.3, 4.6, 4.9, 5.0, 5.2, and 6.7. In Figure 8, three representative ^{1}H NMR EXSY spectra at pH 3.5, 3.7, and 5.0 are shown. Cross signals between H2 of the complex and H2 of the uncomplexed ligand were observed; these indicate exchange between free ligand and complex. Increasing the pH to 4.3 and higher produced EXSY spectra in which the complex−ligand cross peaks were dramatically lower than in the spectrum at pH 3.7.

The chemical shifts for the free ligand and the complex varied with pH only over a small chemical shift range (Figure 6), so no observable changes in cross-signal intensities due to chemical shift differences would be anticipated. The cross-peak volume intensities changed as a function of pH. In Figure 9 the total exchange volume intensities are represented by the ratio of total exchange volume integral (for H2 in the complex compared to H2 in the free ligand) to the total diagonal signal volume integrals. The data shown were recorded for solutions with the concentration ranges used in Figure 8, although selected samples in higher concentrations were also recorded with similar results. The exchange rate is least in the pH region 4−7.

Support for the results shown in Figure 9 was sought by recording the ^{13}C EXSY NMR spectra at additional pH values for comparison with the data obtained at pH 3.5. No evidence for exhange in the pH region 4−7 was found (the diagonal signals in these spectra are very strong as anticipated). Below pH 3 the solubility of the ligand was limited, but it was still possible to observe exchange in the ^{13}C EXSY NMR spectrum by examining the slices separately (data not shown). In summary, the ^{13}C NMR data support the ^{1}H NMR data in that exchange at pH 4−7 was not observable, whereas exchange was observed at pH < 4.

Significance of the Differences between $[VO_2(\text{dipic-OH})]^-$ and $[VO_2(\text{dipic})]^-$. Previous studies with the $[VO_2(\text{dipic})]^-$ complex demonstrated the pH-dependent stability and lability of this complex.[25] The $[VO_2(\text{dipic-OH})]^-$ complex exhibits slightly higher stability at neutral pH, extending the stability range of the complex by 0.5−1.0 pH units as compared to $[VO_2(\text{dipic})]^-$. Previously, ligand modifications have been found to modify complex stability but not lability.[24] Thus, the changes observed on comparing the parent complex's pH-lability profile (minimum at 2.5−4.5) to that of $[VO_2(\text{dipic-OH})]^-$ was unexpected. No ligand exchange was observed for $[VO_2(\text{dipic-OH})]^-$ above pH 4, presumably in part because of the decreased lability from 4 to 7 and the fact that only small concentrations of complex exist above pH 7. The hydroxyl group is therefore found to modify *both the lability and stability* of the resulting vanadium(V) complex. This finding suggests that other ligand substitutions will generate complexes with predictable properties.

To date, most of the vanadium complexes that have been reported to have insulin-like properties contain vanadium(IV). The recent observation that the $[VO_2(\text{dipic})]^-$ complex has insulin-like properties suggests that this complex maintains the desirable properties of the vanadium(IV) complexes. These findings are particularly striking in light of the fact that vanadium(V) analogues of $VO(\text{malto})_2$ and kojic acid complexes[35] are found to have no insulin-like effect. Similar observations (activity with V(IV), lack of activity with V(V)) have been made for $V^{IV}O(\text{acac})_2$ and $V^{V}O_2(\text{acac})$ (unpublished results). Recently, in vitro studies have been reported with a large number of vanadium complexes, including vanadium(V) complexes.[36] These studies, using transformed SV 3T3 fibroblasts from mice and nontransformed human fibroblasts (F26),[36] as well as our studies in various in vitro systems (ref 4 and unpublished data), may be important to determine which complexes have insulin-like effects in excess of the effect observed with simple salts. Identification of other vanadium(V) complexes with properties complementary to those of $[VO_2(\text{dipic})]^-$ is also important in the

(35) Yuen, V. G.; Caravan, P.; Gelmini, L.; Glover, N.; McNeill, J. H.; Setyawati, I. A.; Zhou, Y.; Orvig, C. *J. Inorg. Biochem.* **1997**, *68*, 109−116

(36) Rehder, D.; Pessoa J. C.; Geraldes, C. F. G. C.; Castro, M. M. C. A.; Kabanos, T.; Kiss, T.; Meier, B.; Micera, G.; Pettersson, L.; Rangel, M.; Salifoglou, A.; Turel, I.; Wang, D. *J. Biol. Inorg. Chem.* **2002**, *7*, 384−396.

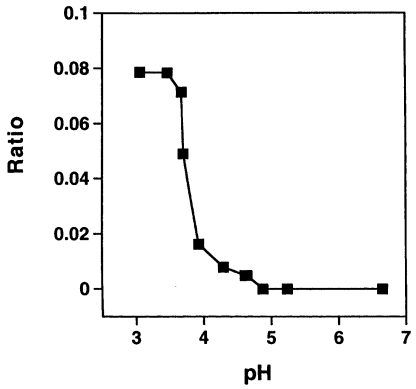

Figure 9. The ratio of total volume integrals of exchange cross signals between complex ($[VO_2(dipic\text{-}OH)]^-$ or $[VO_2(dipic{-}O^-)]^{2-}$) and free ligand and the total diagonal signals obtained from ^1H EXSY NMR spectra vs pH.

attempts to investigate and identify the properties of vanadium complexes that are key to their insulin-like action.

The insulin-like properties of the $[VO_2(dipic)]^-$ complex are of interest for several reasons. The compound is charged, which in principle should hinder absorption. The compound is unstable at the physiological pH of cellular targets. In addition, the compound is labile. It has been proposed that the $[VO_2(dipic)]^-$ complex is reduced to a species that has greater stability at the pH of the cellular target. It has also been proposed that the activity of the complex may be associated with its high stability and relatively low lability at stomach pH.[6] The possibility that the role of the ligand is to ensure passage of complex through the digestive tract before facilitating transport to the site of action can be tested once related complexes have been characterized. The $[VO_2(dipic\text{-}OH)]^-$ complex is such a compound, and studies evaluating the effect of this complex on lowering the elevated glucose levels in appropriate animal model systems are underway.

Acknowledgment. This research was supported by a grant from the National Institute of General Medical Sciences of The National Institutes of Health (to D.C.C.). The X-ray diffractometer was purchased with funds made available by the National Institutes of Health through its Shared Instrumentation Grant Program.

IC0201598